High-temperature studies of grain boundaries in ultrafine grained alloys by means of positron lifetime

R. Würschum,[1,2,*] E. Shapiro,[2] R. Dittmar,[2] and H.-E. Schaefer[2]
[1]*Forschungszentrum Karlsruhe GmbH, Institut für Nanotechnologie, Postfach 3640, D-76021 Karlsruhe, Germany*
[2]*Universität Stuttgart, Institut für Theoretische und Angewandte Physik, Pfaffenwaldring 57, D-70550 Stuttgart, Germany*
(Received 3 April 2000)

Atomic free volumes and vacancies in the ultrafine grained alloys $Pd_{84}Zr_{16}$, Cu 0.1 wt % ZrO_2, and $Fe_{91}Zr_9$ were studied by means of positron lifetime. The thermally stable microstructures serve as a novel type of model system for studying positron trapping and annihilation as well as the thermal behavior of vacancy-sized free volumes over a wide temperature range up to ca. 1200 K by making use of a metallic ^{58}Co positron source. In ultrafine grained Cu the thermal formation of lattice vacancies could be observed. In $Pd_{84}Zr_{16}$ an increase of the specific positron trapping rate of nanovoids and, in addition, detrapping of positrons from free volumes with a mean size slightly smaller than one missing atom in the grain boundaries contributes to a reversible increase of the positron lifetime of more than 60 ps with measuring temperature. In $Fe_{91}Zr_9$ similar linear high-temperature increases of the positron lifetime are observed in the nanocrystalline and the amorphous state. The question of thermal vacancy formation in grain boundaries is addressed taking into account the different types of interface structures of the present alloys.

I. INTRODUCTION

Atomic free volumes and diffusion in grain boundaries are closely linked and represent key issues for high-temperature materials properties, such as plasticity, sintering, or structural stability. This is particularly true for ultrafine grained materials which contain a high number of grain boundaries.[1,2] Computer simulations (see, e.g., Ref. 3) and measurements of the pressure dependence of atomic diffusion[4] indicate that grain-boundary self-diffusion in metals is mediated by thermal vacancies similar to crystals (for details, see Ref. 5). However, so far, no direct evidence of thermal defect formation in grain boundaries, for instance, by means of positron lifetime spectroscopy, exists.

Positron lifetime measurements at high temperatures have proved a valuable tool for studying thermal formation of lattice vacancies in metals[6] and intermetallic compounds.[7] The technical requirements now are achieved in order to perform the same kind of studies for defects in grain boundaries, the results on which are presented in the present paper. These technical requirements comprise the preparation of ultrafine grained alloys, i.e., systems with a high number of grain boundaries, which show sufficient thermal stability[8,9] and the concomitant development of appropriate techniques for measuring the positron lifetime at high temperatures in these systems (see Sec. II).

The present first systematic studies of this kind aim at the question of whether the formation of atomic defects in grain boundaries under thermal equilibrium conditions at high temperatures can be detected, e.g., by the specific technique of positron lifetime spectroscopy. A detection of these thermal defects might be hampered from a principal point of view by a strong relaxation of the thermal vacancies in grain boundaries as indicated by computer simulations.[10,11] In addition, as outlined below, a competitive trapping of positrons at structurally free volumes in the interfaces[12] may have to be taken into consideration. Besides the topic of thermal defect formation in grain boundaries, thermally stable ultrafine grained alloys may serve as novel model systems in order to study the temperature dependence of the specific trapping rate of extended defects, like nanovoids, over a wide temperature range. Such data, which are of general interest for the understanding of the positron annihilation characteristics in condensed matter, were so far primarily gained from metals after particle irradiation and restricted to a low-temperature regime (see, e.g., Refs. 13–19). Finally, high-temperature measurements of the positron lifetime in ultrafine grained alloys may further elucidate the character of the different positron trapping sites in these structural complex systems by means of the different temperature dependencies of the positron trapping rates.

Ultrafine grained metallic systems with three different types of microstructures and grain boundaries were studied: (i) nanocrystalline (n-)$Fe_{91}Zr_9$ prepared by crystallization from melt-spun amorphous ribbons which exhibits a residual amorphous matrix in the interfaces;[12,20,21] (ii) ball-milled nanocrystalline $Pd_{84}Zr_{16}$ stabilized by Zr segregation at the grain boundaries;[8] (iii) microcrystalline (mc-)Cu with ZrO_2 precipitates prepared by severe plastic deformation.[9]

After a brief description of the experimental procedure (Sec. II), the results of the high-temperature positron lifetime measurements are presented (Sec. III) and discussed (Sec. IV).

II. EXPERIMENTAL PROCEDURE

Nanocrystalline $Fe_{91}Zr_9$ was prepared by crystallization of melt-spun amorphous ribbons at 873 K for 48 h under high vacuum conditions. This thermal treatment results in a two-phase microstructure of α-Fe and Fe_2Zr nanocrystallites with a mean grain size d of ca. 30 nm.[20,22]

Nanocrystalline $Pd_{84}Zr_{16}$ was prepared by mechanically alloying powder mixtures of Zr (99.7%) and Pd (99.9%) in a

SPEX 8000 shaker mill under Ar atmosphere for 24 h.[8] The contents of the light impurities H, N, and O was 2.4, 0.2, and 2.4 at. %, respectively, as determined by hot-extraction analysis. The concentration of Fe was below 1 at. %. For the subsequent handling with the positron sources the ball-milled powder was compacted in high vacuum under uniaxial pressure of ca. 1.8 GPa into disk-shaped pellets.

For the preparation of microcrystalline Cu with ZrO_2 precipitates (Cu 0.1 wt % ZrO_2) a Cu-Zr single crystal was internally oxidized and subsequently deformed severely by the technique of equichannel angular pressing as described in more details elsewhere (see Ref. 9).

The positron lifetime measurements were performed by means of a $\gamma\gamma$-coincidence spectrometer[6] with a ^{58}Co positron source.[23] The metallic ^{58}Co positron source was prepared from a $^{58}CoCl_2$ starting material which was initially deposited on a ribbon of the specimen material, reduced in a H_2 atmosphere at 540 K for 1 h and subsequently annealed under high vacuum (5×10^{-6} mbars) at the reduction temperature (n-$Fe_{91}Zr_9$) or at higher temperatures (n-$Pd_{84}Zr_{16}$: 770 K; mc-Cu/ZrO_2: 640 K). For each material system the specimen piece with the ^{58}Co positron source was stacked between identical specimen platelets in a metal container and sealed off in a quartz ampoule under high vacuum. By means of this specimen-source arrangement measuring temperatures of up to 1173 K were realized in the present experiments without evaporation or loss of activity.

The positron lifetime spectra with a time resolution (FWHM, full width at half maximum) of 250–285 ps and $0.6-2\times10^6$ coincidence counts were analyzed by numerical standard techniques (see Ref. 6). The measurements of the temperature dependence of the positron lifetime were performed after preannealing at the maximum measuring temperature in order to avoid structural changes during the measuring runs.

III. EXPERIMENTAL RESULTS

In $Fe_{91}Zr_9$ single-component positron lifetime spectra with similar linear temperature variations of the mean positron lifetime $\bar{\tau}$ occur in the amorphous and in the nanocrystalline state after preannealing at $T_a=973$ K (Fig. 1). The single positron lifetime $\bar{\tau}=163$ ps (ambient temperature) characterizes free volumes slightly smaller than a lattice vacancy taking into account the positron lifetime $\tau_V=175$ ps of lattice vacancies in α-Fe (see Refs. 12 and 20). Grain coarsening up to approx. 1 μm upon annealing at $T_a=1173$ K (Ref. 24) gives rise to a decrease of the positron lifetime to 124 ps.

In the case of $Pd_{84}Zr_{16}$ the high thermal stability due to the Zr segregation enables positron lifetime measurements of a submicrocrystalline structure up to temperatures as high as 1173 K. An average crystallite size of 120 nm is observed *after* the high-temperature positron lifetime measurements (Fig. 2). A substantial linear increase of the mean positron lifetime $\bar{\tau}$ by more than 60 ps occurs between ambient temperature and the maximum temperature (Fig. 3). This increase is fully reversible since after the various high-temperature measuring runs identical values $\bar{\tau}$ at ambient temperatures are observed (see caption of Fig. 3 for the sequence of data points). The positron lifetime spectroscopy shows that the increase of $\bar{\tau}$ is due to the increase of the ratio

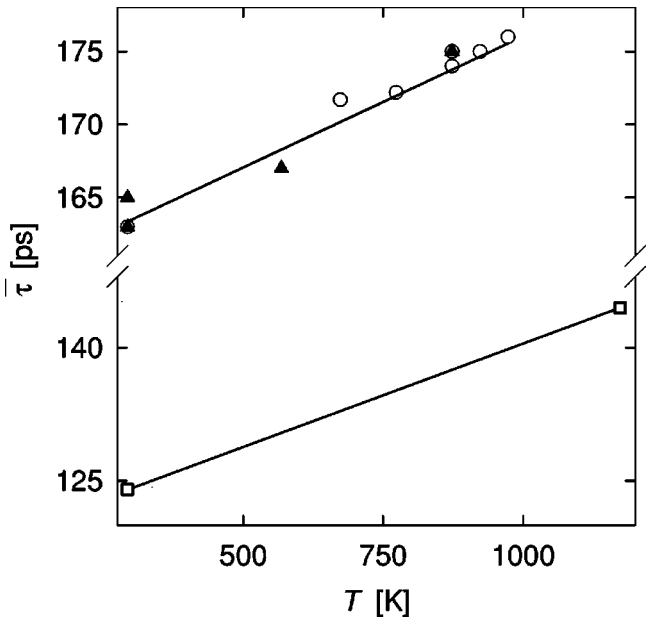

FIG. 1. Positron lifetime $\bar{\tau}$ measured at the temperature T in $Fe_{91}Zr_9$ in the amorphous state (▲), in the nanocrystalline state after annealing at $T_a=973$ K (○), and in the microcrystalline state after annealing at $T_a=1173$ K (□).

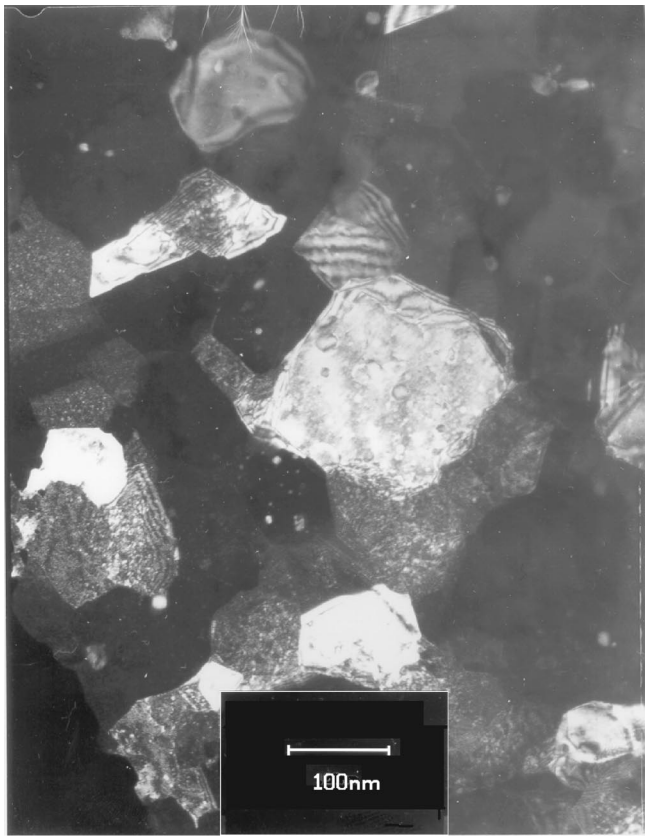

FIG. 2. Transmission electron micrograph (dark field) of the nanocrystalline $Pd_{84}Zr_{16}$ specimen after high-temperature measurements of the positron lifetime (cf. Fig. 3). Maximum measuring temperature $T=1173$ K.-

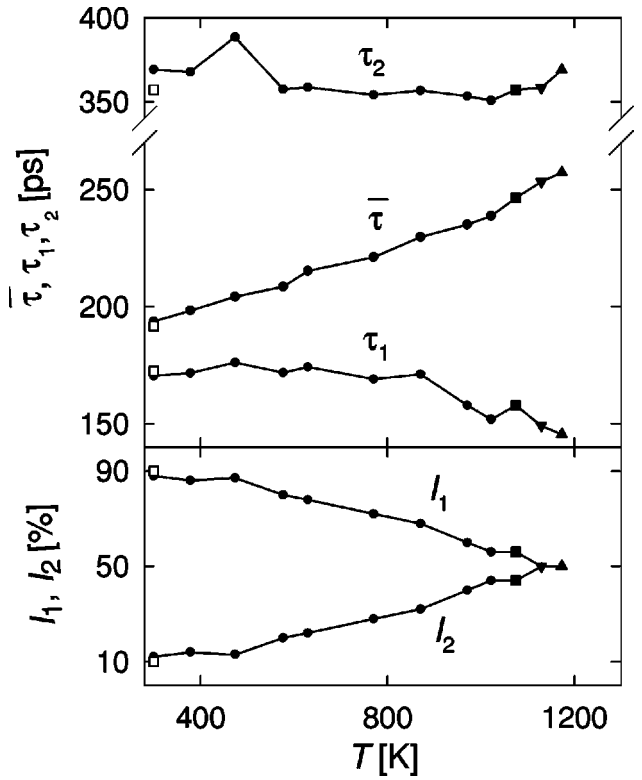

FIG. 3. Mean positron lifetime $\bar{\tau}$ and positron lifetime components τ_1, τ_2 with relative intensities I_1, I_2 measured on n-$Pd_{84}Zr_{16}$ at the temperature T during (■) and after annealing at 1075 K (●) and during annealing at 1129 K (▼), and 1173 K (▲). Identical $\bar{\tau}$ values are observed at ambient temperature after annealing at 1075 K and 1173 K. The □ denote the values prior to the high-temperature measurements.

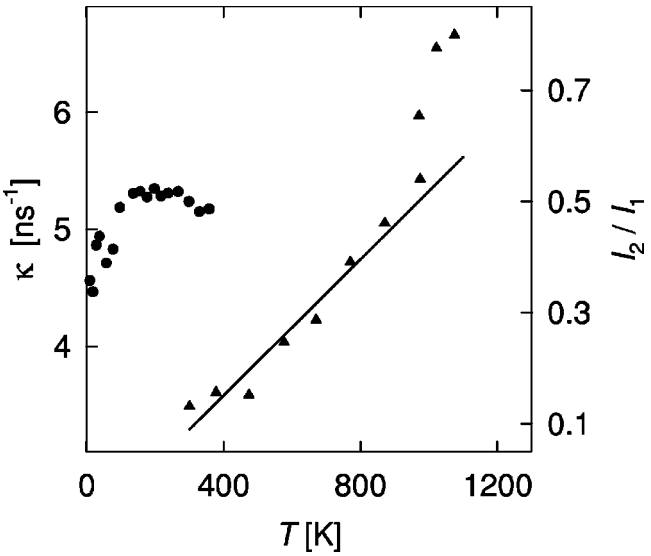

FIG. 4. Ratio $I_2/I_1=(\sigma_{\text{void}} C_{\text{void}})/(\sigma_1 C_1)$ [Eq. (1), ▲] of the relative intensities of the positron lifetime components in n-$Pd_{84}Zr_{16}$ (cf. Fig. 3) in comparison to literature data of the positron trapping rate κ of voids in neutron-irradiated Mo (●, Ref. 14). $\kappa=\sigma_{void} C_{void}$ in the transition-limited regime for $T<200$ K (see text). Measuring temperature T.

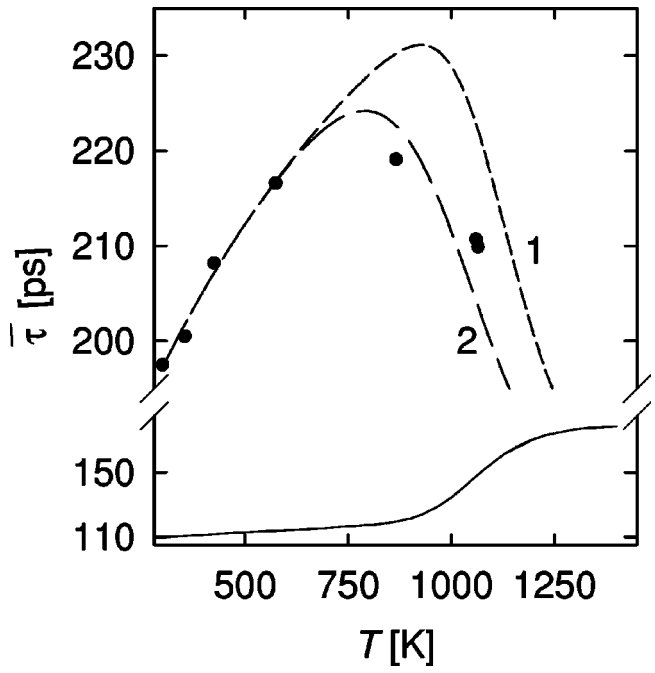

FIG. 5. Mean lifetime $\bar{\tau}$ in ultrafine grained Cu 0.1 wt % ZrO_2 after annealing at 1060 K (●). The curves denote fits taken into account reaction controlled at interfaces and nanovoids, thermal vacancy formation in crystallites (curve 1) and, in addition, thermal vacancy formation in the grain boundaries (curve 2); see text for details. The solid line denotes the temperature dependence of $\bar{\tau}$ in coarse-grained pure Cu arising from positron trapping and annihilation in thermal lattice vacancies (Ref. 6).

I_2/I_1 of the relative intensities of the positron lifetime components τ_1 and τ_2 (Figs. 3 and 4).

In Cu 0.1 wt % ZrO_2 the mean positron lifetime $\bar{\tau}$ at first increases reversibly similar as in $Pd_{84}Zr_{16}$ whereas for temperatures above 900 K a reversible decrease of $\bar{\tau}$ occurs (Fig. 5). Due to the reduced statistical accuracy, only the mean value of the positron lifetime is given. A transmission electron micrograph after annealing at 813 K shows a microcrystalline grain structure with a broad grain size distribution ranging from some 100 nm to above 1 μm.

IV. DISCUSSION

An overview of the high-temperature variation of the positron lifetime in the various ultrafine grained alloys including data from recent studies of nanocrystalline $Fe_{73.5}Si_{13.5}B_9Nb_3Cu_1$ (Ref. 25) is given in Fig. 6. As discussed in more detail below, the rather different behavior of the various alloys arise from the different types of trapping sites each of which is characterized by a positron trapping rate with a different temperature dependence. The following temperature dependencies have to be taken into account:

- A strong increase of the specific trapping rate of nanovoids with increasing temperature (see Sec. IV B). These structural elements are present in the mechanically prepared alloys ($Pd_{84}Zr_{16}$, Cu 0.1 wt. % ZrO_2) but not in the nanocrystalline alloys crystallized from amorphous precursors and containing an amorphous intergranular phase (see Sec. IV A).

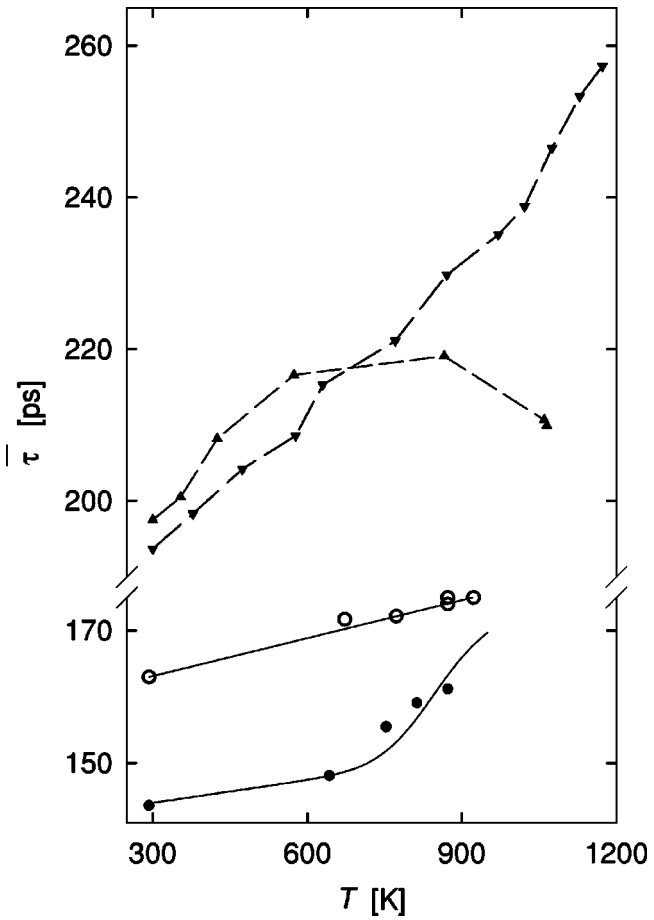

FIG. 6. Overview of high-temperature positron lifetime measurements on ultrafine grained alloys. Mean positron lifetime $\bar{\tau}$ measured on $Pd_{84}Zr_{16}$ (▼, cf. Fig. 3) after annealing at 1173 K, on Cu 0.1 wt % ZrO_2 (▲, cf. Fig. 5) after annealing to 1060 K, on $Fe_{91}Zr_9$ (○, cf. Fig. 1) after annealing at 973 K, and on $Fe_{73.5}Si_{13.5}B_9Nb_3Cu_1$ (●, Ref. 25) after annealing at 873 K.

- A competitive positron trapping and annihilation at thermally formed vacancies (positron lifetime τ_V) in the crystallites which gives rise to a high-temperature decrease or increase of $\bar{\tau}$ in alloys with $\bar{\tau} > \tau_V$ (Cu 0.1 wt. % ZrO_2) or $\bar{\tau} < \tau_V$ ($Fe_{73.5}Si_{13.5}B_9Nb_3Cu_1$), respectively (see Sec. IV D).
- A thermally activated detrapping of positrons from shallow traps at densely packed interfaces in $Pd_{84}Zr_{16}$ and in $Fe_{91}Zr_9$ (see Sec. IV C).

The question of thermal grain boundary vacancies is considered in Sec. IV D.

A. Variation of the positron lifetime with the microstructure

The variation of the positron lifetime in ultrafine grained metals and alloys with the technique used for synthesis has been a subject of comprehensive studies previously (for reviews see Refs. 12 and 21). The most prominent feature pertains to nanovoids as characterized by a long positron lifetime component τ_2 exceeding 300 ps ($Pd_{84}Zr_{16}$, see Fig. 3) which occur in all types of nanocrystalline materials except in *n* alloys prepared by crystallization from the amorphous state such as *n*-$Fe_{91}Zr_9$ and *n*-$Fe_{73.5}Si_{13.5}B_9Nb_3Cu_1$ (Fig. 6). In the latter type of *n* alloys positrons are quantitatively trapped and annihilated in interfacial free volumes slightly smaller than a lattice vacancy. These free volumes may be ascribed to a residual amorphous matrix between the crystallites since free volumes of identical size are found in the initial melt-spun amorphous state.[12,20,25]

In ball-milled *n*-$Pd_{84}Zr_{16}$, in addition to the component $\tau_2 = 360$ ps characteristic for nanovoids, a component $\tau_1 = 175$ ps occurs (Fig. 3). This value is similar to the positron lifetime in Zr-rich amorphous alloys ($\tau_{amorph} = 182$ ps, Ref. 26) but lower than the positron lifetime in lattice vacancies in crystalline Zr ($\tau_V = 219$ ps, see Ref. 26). Therefore the component τ_1 is ascribed to free volumes with a mean size slightly smaller than one missing atom in the Zr-enriched grain boundaries. The attribution of τ_1 to interfacial free volumes rather than to vacancies in the crystallites is supported by the thermal stability of this component above temperatures where crystal vacancies anneal out (Fig. 3) and by the correlation between the intensity of this component and the crystallite size as reported earlier on a ball-milled Pd-Zr sample with similar composition.[27]

In mc-Cu a high value of the mean positron lifetime $\bar{\tau}$ similar as in *n*-$Pd_{84}Zr_{16}$ occurs indicating positron trapping as well. Positron lifetime spectroscopy in undoped Cu prepared by severe plastic deformation reveals two positron lifetime components characteristic for vacancy-type free volumes and nanovoids.[20]

B. Temperature dependence of the specific positron trapping rate of nanovoids

The substantial increase of the mean positron lifetime in *n*-$Pd_{84}Zr_{16}$ and the initial linear $\bar{\tau}$ increase in mc-Cu with increasing temperature (cf. Fig. 6) primarily arise from the increase of the specific trapping rate of nanovoids as outlined in the following. In the case of saturation trapping of positrons in nanocrystalline materials, the intensity ratio

$$\frac{I_2}{I_1} = \frac{\sigma_{void} C_{void}}{\sigma_1 C_1} \tag{1}$$

of the components τ_2 and τ_1 (see Fig. 4) is given by the ratio of the positron trapping rates $\sigma_i C_i$ of nanovoids and vacancy-type free volumes, respectively, where σ_i denotes the specific positron trapping rate and C_i the concentration of the particular defect type *i*. A reversible increase of the nanovoid concentration (C_{void}) with temperature can be ruled out. Therefore we adopt at first the picture that the increase of I_2/I_1 exclusively is due to an increase of the specific trapping rate σ_{void} of nanovoids. This is also supported by the fact that in crystallized *n* alloys without nanovoids the increase of $\bar{\tau}$ with temperature is reduced (cf. Fig. 6). An additional contribution to the I_2/I_1 increase arising from a decrease of $\sigma_1 C_1$ will be discussed in the next section (Sec. IV C).

A linear increase of the specific trapping rate σ_{void} with temperature is known already from studies of irradiation-induced nanovoids in metals[13–19] (e.g., see Fig. 4, ●, for $T < 200$ K) and is considered to arise from the temperature dependence of the elastic scattering of positrons at voids.[28] However, the present results on nanocrystalline $Pd_{84}Zr_{16}$ dif-

fer substantially from the former data since the linear increase of $\sigma_{void} C_{void}$ (see Fig. 4, ▲, with $\sigma_1 C_1 = \text{const}$) is extended to substantially higher temperatures. This indicates that the trapping process at nanovoids in the nanocrystalline alloy is transition limited within the whole temperature range whereas for irradiated metals the trapping process becomes diffusion limited at elevated temperatures. The transition to the diffusion-limited regime in the irradiated samples arises from the lower nanovoid concentration C_{void} and the larger specific positron trapping rates σ_{void} due to the larger void sizes.[15] This is confirmed by the following estimation of the values of C_{void} and σ_{void} of the two types of experiments. E.g., in the given case of neutron-irradiated Mo with voids of the size of 2.6 nm and a low concentration of 8×10^{-8}, high values $\sigma_{void} > 10^{16}$ s^{-1} are estimated from the measured trapping rates $\sigma_{void} C_{void}$ (Fig. 4, ●, Ref. 14). In n-$Pd_{84}Zr_{16}$ the smaller nanovoid size of 10–15 missing atoms (nanovoid diameter $\simeq$0.5–0.8 nm) is considered to be associated with lower values $\sigma_{void} \simeq 10^{15}$ s^{-1}.[13,15] On the other hand, the nanovoid concentration C_{void} in n-$Pd_{84}Zr_{16}$ is higher than the concentration of irradiation-induced voids. In the case of transition-limited positron trapping, C_{void} can be deduced from the ratio I_2/I_1 by means of an estimate of the trapping rate in grain boundaries according to the relation $\sigma_1 C_1 = 6\,\alpha\, d^{-1}$.[29] With the specific trapping rate $\alpha = 4.2\times10^2$ m s^{-1} of grain boundaries deduced from the correlation of I_1 and d upon crystallite growth,[27] the crystallite size $d = 120$ nm as given above, and $\sigma_{void} \simeq 10^{15}$ s^{-1}, a concentration $C_{void} = 2\times10^{-6}$ is derived from the ratio I_2/I_1 at ambient temperature which is indeed more than order of magnitude higher than in the irradiated sample.

From the linear increase of I_2/I_1, a temperature coefficient $\beta = 6.5\times10^{-3}$ K^{-1} of $\sigma_{void} \propto 1+\beta\Delta T$ can be determined (Fig. 4, straight line). A similar value $\beta = 6\times10^{-3}$ K^{-1} is derived for mc-Cu from the initial increase of

$$\overline{\tau} = \frac{\tau_1\,\sigma_1\,C_1 + \tau_2\,\sigma_{void}\,C_{void}}{\sigma_1 C_1 + \sigma_{void} C_{void}} \qquad (2)$$

below 600 K (Figs. 5 and 6) assuming reaction-controlled saturation trapping of positron at the two types of traps with the time constants $\tau_1 = 180$ ps and $\tau_2 = 300$ ps as in undoped Cu after severe plastic deformation.[20] These values of β are similar to those usually found for larger voids induced by irradiation[13–19] although β is expected to decrease with the void diameter.[28] This indicates that, in addition to the intrinsic temperature dependence of σ_{void}, a decrease of $\sigma_1 C_1$ with increasing temperature contributes to the strong increase of I_2/I_1 with T (see Sec. IV C).

C. Thermal detrapping from interfacial free volumes

As discussed in the previous section, the increase of $\overline{\tau}$ or I_2/I_1 in n-$Pd_{84}Zr_{16}$ (and mc-Cu) with temperature cannot exclusively be attributed to an increase of σ_{void} but, in addition, is due to a decrease of the trapping rate $\sigma_1 C_1$ at grain boundaries at elevated temperatures. Likewise, in n-$Fe_{91}Zr_9$ (Fig. 1) the linear temperature coefficient $\gamma = 10^{-4}$ K^{-1} of the positron lifetime $\overline{\tau} = \overline{\tau}_{293K}[1+\gamma(T-293\ \text{K})]$ in the interfacial free volumes is higher than that which is usually observed for a vacancy-trapped state as, for example, for structural vacancies in NiAl where a value of $\gamma = 10^{-5}$ K^{-1} is found (see Fig. 3 of Ref. 7). Both effects, namely the decrease of $\sigma_1 C_1$ and the enhanced temperature coefficient γ, most likely are caused by a thermal detrapping of positrons from shallow traps similar to that in amorphous alloys.[30]

This becomes clear by recalling that the free volume size in the grain boundaries, as characterized by the component τ_1 in n-$Pd_{84}Zr_{16}$ or by the single component $\overline{\tau}$ in n-$Fe_{91}Zr_9$, has to be regarded as a mean value (see Ref. 12). Positrons weakly bound to smaller free volumes, i.e., shallow traps, may escape by thermal activation at elevated temperature and be retrapped at larger free volumes which are capable of tightly binding positrons. By such a process the mean size of interfacial traps probed by positrons is shifted towards higher values which can explain the observed increase of the single component $\overline{\tau}$ in n-$Fe_{91}Zr_9$. In n-$Pd_{84}Zr_{16}$, positrons can be retrapped in adjacent nanovoids in the grain boundaries giving rise to a decrease of $\sigma_1 C_1$ and an increase of $\sigma_{void} C_{void}$. In the framework of this interpretation, the decrease of $\sigma_1 C_1$ with temperature is due to the increasing fraction of free volumes from which detrapping of positrons may occur.

In n-$Pd_{84}Zr_{16}$, τ_1 is constant within the present uncertainties ($\Delta\tau_1 \simeq \pm 10$ ps) up to ca. 800 K (Fig. 3) although the effective mean size of free volumes increases due to detrapping of positrons from small free volumes as outlined above. On the one hand, this may be due to partial positron annihilation in the free state of the crystallites upon detrapping which, in contrast to n-$Fe_{91}Zr_9$, has to be to be taken into account for n-$Pd_{84}Zr_{16}$ due to the larger crystallite size. In addition, a detrapping and subsequent retrapping in the traps τ_2 may increase the rate of removal of positrons from the traps τ_1. Both effects would tend to decrease the average value τ_1 and therefore counterbalance a possible τ_1 increase due to the increase of the effective free volume size. The decrease of τ_1 observed above 800 K (Fig. 3) implies for this model that the former processes become dominant at high temperatures.

D. Thermal formation of lattice vacancies and question of thermal vacancy formation in grain boundaries

Experimental evidence of thermal vacancy formation in a nanocrystalline material was recently obtained by Würschum *et al.* for n-$Fe_{73.5}Si_{13.5}B_9Nb_3Cu_1$ prepared by crystallization.[25] In this nanocomposite structure, $D0_3$-type $Fe_{80}Si_{20}$ nanocrystallites are embedded in an amorphous intergranular matrix. From the high-temperature increase of the mean positron lifetime $\overline{\tau}$ (see Fig. 6) a vacancy-formation enthalpy $H_V^F = 1.1$ eV as in single-crystalline $D0_3$-$Fe_{79}Si_{21}$ could be derived[25] indicating that in this case thermal vacancy formation is detected in the nanocrystallites rather than in the intergranular amorphous matrix or in the interfaces between the crystallites and the amorphous phase.

As discussed in the following, thermal formation of lattice vacancies is also found in the present studies of ultrafine grained Cu (see Fig. 5). However, the variation of $\overline{\tau}$ due to thermal vacancy formation differs from the well-known behavior of coarse-grained metals. In fact, thermal lattice va-

cancies in ultrafine grained Cu act as additional trapping centers at high temperatures which reduces the effective trapping rate in nanovoids and therefore gives rise to the reversible high-temperature decrease of $\overline{\tau}$ (see Fig. 5). According to earlier positron lifetime measurements on coarse-grained pure Cu (Ref. 6) positron trapping and annihilation in thermal lattice vacancies starts to occur at about 900 K (see solid line in Fig. 5). Thermal vacancy formation in mc-Cu can be taken into account by means of an extension of Eq. (2). In the framework of this simple model the mean positron lifetime

$$\overline{\tau}=\frac{\tau_1\sigma_1C_1+\tau_2\sigma_{\mathrm{void}}C_{\mathrm{void}}+\tau_{\mathrm{V}}\sigma_{\mathrm{V}}C_{\mathrm{V}}}{\sigma_1C_1+\sigma_{\mathrm{void}}C_{\mathrm{void}}+\sigma_{\mathrm{V}}C_{\mathrm{V}}} \tag{3}$$

is the trapping-rate averaged value of the positron lifetimes in interfaces (τ_1), nanovoids (τ_2), and thermal lattice vacancies (τ_{V}) which compete as positron traps. The high-temperature decrease of $\overline{\tau}$ depicted by curve 1 in Fig. 5 is calculated assuming $\tau_{\mathrm{V}}=180$ ps and making use of the thermal vacancy characteristics derived for coarse-grained Cu (Ref. 6), i.e., a vacancy-formation enthalpy $H_{\mathrm{V}}^{\mathrm{F}}=1.42$ eV with a pre-exponential factor $\sigma_{\mathrm{V}}\exp(S_{\mathrm{V}}^{\mathrm{F}}/k_{\mathrm{B}})=3.8\times10^{16}\ \mathrm{s}^{-1}$ where $S_{\mathrm{V}}^{\mathrm{F}}$ denotes the vacancy-formation entropy. The trapping rate of the interfacial free volumes is calculated by means of the relation $\sigma_1C_1=6\alpha d^{-1}$ (see Sec. IV B) using a mean crystallite size $d=250$ nm. The temperature-dependent trapping rate of nanovoids is taken from the initial $\overline{\tau}$ increase as outlined in Sec. IV B [see Eq. (2)].

A comparison with the experimental data shows that the high-temperature decrease of $\overline{\tau}$ occurs at lower temperatures than predicted by the vacancy formation parameters of crystalline Cu (curve 1, Fig. 5).[31] An unambiguous assessment whether this shift is due to thermal grain boundary vacancies is, however, hampered by the numerous assumptions underlying the present simple model. Nevertheless, it is worthwhile to point out that a better fit can be achieved by introducing in Eq. (3) a second thermal vacancy-type trap ($\tau_{\mathrm{V},2}$) with a formation enthalpy $H_{\mathrm{V},2}^{\mathrm{F}}$ which is lower than that of crystal vacancies as should be the case for thermal grain boundary vacancies.[3] This is shown by curve 2 in Fig. 5 which is obtained with $\tau_{\mathrm{V}2}=170$ ps, $H_{\mathrm{V},2}^{\mathrm{F}}=0.5\times H_{\mathrm{V}}^{\mathrm{F}}=0.7$ eV, and a pre-exponential factor $\sigma_{\mathrm{V}}\exp(S_{\mathrm{V}}^{\mathrm{F}}/k_{\mathrm{B}})=3\times10^{13}\ \mathrm{s}^{-1}$.

In contrast to mc-Cu, thermal vacancy formation in grain boundaries of n-$Pd_{84}Zr_{16}$ presumably can be ruled out due to the following considerations. In undoped grain boundaries of Pd, thermal grain boundary vacancies are to be expected in the temperature range studied here, taking into account the onset temperature of ~1150 K (Ref. 6) of positron trapping in lattice vacancies and the argument used above that the formation enthalpy $H_{\mathrm{V}}^{\mathrm{F}}$ of vacancies in grain boundaries should be well below that of lattice vacancies[3] (c-Pd: $H_{\mathrm{V}}^{\mathrm{F}}=1.85$ eV, Ref. 6). The present measurements show an increase of the ratio $(\sigma_{\mathrm{void}}C_{\mathrm{void}})/(\sigma_1C_1)$ of the positron trapping rates and therefore no evidence for thermal vacancy formation in the grain boundaries which should be manifested in the detection of an increase of C_1. More accurately, as outlined in Sec. IV C there are indication that σ_1C_1 decreases with temperature. Although it may not be excluded that a detection of thermal vacancies in grain boundaries might be hampered by, e.g., a strong relaxation of the vacancy,[10,11] it appears most likely that the formation of thermal vacancies in the grain boundaries of nanocrystalline $Pd_{86}Zr_{14}$ alloys is suppressed by the segregation-induced substantial decrease of the specific grain-boundary energy.[8] As known from grain-boundary diffusion studies, a low interfacial excess energy due to doping is associated with a strong reduction of the grain boundary diffusivity (see, e.g., Sn-doped Fe, Ref. 32). A reduced diffusivity represents a strong evidence for a reduced thermal vacancy formation in grain boundaries upon doping.

This consideration may similarly pertain to the nanocrystalline alloys $Fe_{73.5}Si_{13.5}B_9Nb_3Cu_1$ and $Fe_{91}Zr_9$ crystallized from the amorphous state where the interfacial diffusivity is also rather slow compared to undoped grain boundaries due to the amorphous intergranular phase.[22,25] As outlined in Sec. IV C the enhanced temperature coefficient γ of the positron lifetime in n-$Fe_{91}Zr_9$ is considered to reflect thermal detrapping of positrons as in amorphous alloys. Due to the following reasons it appears unlikely that this enhanced increase of $\overline{\tau}$ with temperature arises from thermal defect formation in the interfaces. On the one hand, the enhanced increase $\overline{\tau}$ is linear over a wide temperature range (Fig. 1) in contrast to the $\overline{\tau}$ characteristics expected for positron trapping at thermally formed defects. On the other hand, the kind of temperature dependence found in n-$Fe_{91}Zr_9$ was observed in amorphous alloys also below ambient temperature[30,33] where thermal defect formation can be ruled out.

V. SUMMARY AND CONCLUSIONS

Structurally stable nano- and microcrystalline materials serve as a novel type of model system for studying positron trapping and annihilation over a wide temperature range. By means of the metallic ^{58}Co positron source positron lifetime measurements up to ca. 1200 K could be performed on various metallic systems with different types of microstructures and interfaces. These kind of studies enable the detection of thermal lattice vacancies in crystallites of ultrafine grained materials as found previously in n-$Fe_{73.5}Si_{13.5}B_9Nb_3Cu_1$ (Ref. 25) and in the present studies on ultrafine grained Cu. Due the presence of nanovoids, the variation of $\overline{\tau}$ in mc-Cu upon thermal vacancy formation differs from the well-known behavior of coarse-grained metals. The same type of $\overline{\tau}$ variation has been found in ball-milled n-Fe_3Si quite recently[34] supporting the present interpretation in the case of mc-Cu.

In $Pd_{84}Zr_{16}$ and Cu an increase of the specific positron trapping rate of nanovoids with increasing temperature is observed in measurements which are extended to substantially higher temperatures than in earlier studies of irradiation-induced voids. In addition, a thermally activated detrapping of positrons from shallow traps in grain boundaries contributes to the strong increase of the mean positron lifetime $\overline{\tau}$ with temperature. A distinction of the various trapping processes, e.g., of nanovoids and thermal vacancies, is enabled by their different temperature dependencies. The question of thermal vacancy formation in grain boundaries for which preliminary hints were found in the case of Cu

demands for further clarification. According to the present studies and the theoretical model of positron trapping at grain boundaries[29] an ideal microstructure for this kind of measurements should be free of nanovoids and exhibit a narrow crystallite size distribution in the range of several 100 nm which allows the detection of thermal defect formation in grain boundaries by means of a temperature-dependent fraction of positrons annihilated in the free state in the crystallites.

ACKNOWLEDGMENTS

The authors are indebted to M. Kelsch (Max-Planck-Institut für Metallforschung, Stuttgart) for the TEM characterization as well as to C. E. Krill, H. Ehrhardt (Univ. des Saarlandes, Saarbrücken), and A. Lebedev (Ioffe-Institute, St. Petersburg) for supplying the ultrafine grained Pd-Zr and Cu 0.1 wt % ZrO_2 samples, respectively. Financial support by Deutsche Forschungsgemeinschaft is appreciated.

*Corresponding author. Present address: Technische Universität Graz, Institut für Technische Physik, Petersgasse 16, A-8010 Graz, Austria. Email address: wuerschum@int.fzk.de

[1] R. Würschum, U. Brossmann, and H.-E. Schaefer, in *Nanostructured Materials: Processing, Properties, and Potential Applications*, edited by C. C. Koch (in press).

[2] R. Würschum, La Revue de Métallurgie - CIT/Science et Génie des Matériaux **96**, 1547 (1999).

[3] R. W. Balluffi, T. Kwok, P. D. Bristowe, A. Brokman, P. S. Ho, and S. Yip, Scr. Metall. **15**, 951 (1981).

[4] G. Martin, D. A. Blackburn, and Y. Adda, Phys. Status Solidi **23**, 223 (1967).

[5] I. Kaur, Y. Mishin, and W. Gust, *Fundamentals of Grain and Interphase Boundary Diffusion* (John Wiley, Chichester, 1995), p. 435.

[6] H.-E. Schaefer, Phys. Status Solidi **102**, 47 (1987).

[7] H.-E. Schaefer, K. Frenner, and R. Würschum, Intermetallics **7**, 277 (1999).

[8] C. E. Krill, R. Klein, S. Janes, and R. Birringer, Mater. Sci. Forum **179-181**, 443 (1995); C. E. Krill, H. Ehrhardt, and R. Birringer, in *Chemistry and Physics of Nanostructures and Related Non-Equilibrium Materials*, edited by E. Ma, B. Fultz, R. Shull, J. Morral, and P. Nash (Minerals, Metals & Materials Soc., Warrendale, PA, 1997), p. 115.

[9] A. B. Lebedev, S. A. Pulnev, V. I. Kopylov, Yu A. Burenkov, V. V. Yetrov, and O. V. Vylegzhanin, Scr. Mater. **35**, 1077 (1996).

[10] H. Hahn and H. Gleiter, Acta Metall. **29**, 601 (1981).

[11] P. D. Bristowe, A. Brokman, F. Spaepen, and R. W. Balluffi, Scr. Metall. **14**, 943 (1980).

[12] R. Würschum and H.-E. Schaefer, in *Nanomaterials: Synthesis, Properties, and Applications*, edited by A. S. Edelstein and R. C. Cammarata (IOP, Bristol, 1996), p. 277.

[13] R. M. Nieminen, J. Laakkonen, P. Hautojärvi, and A. Vehanen, Phys. Rev. B **19**, 1397 (1979).

[14] M. D. Bentzon and J. H. Evans, J. Phys.: Condens. Matter **2**, 10 165 (1990).

[15] M. Eldrup and K. O. Jensen, Phys. Status Solidi A **102**, 145 (1987).

[16] M. D. Bentzon, S. Linderoth, and K. Petersen, in *Positron Annihilation*, edited by P. C. Jain, R. M. Singru, and K. P. Gopinathan (World Scientific, Singapore, 1985), p. 485.

[17] P. J. Schultz, K. G. Lynn, I. K. MacKenzie, Y. C. Jean, and C. L. Snead, Jr., Phys. Rev. Lett. **44**, 1629 (1980).

[18] B. Pagh, H.-E. Hansen, B. Nielsen, G. Trumpy, and K. Petersen, in *Positron Annihilation*, edited by P. G. Coleman, S. C. Sharma, and L. M. Diana (North-Holland, Amsterdam, 1982), p. 398.

[19] S. Linderoth, M. D. Bentzon, H. E. Hansen, and K. Petersen (Ref. 16), p. 494.

[20] R. Würschum, W. Greiner, R. Z. Valiev, M. Rapp, W. Sigle, O. Schneeweiss, and H.-E. Schaefer, Scr. Metall. Mater. **25**, 2451 (1991).

[21] R. Würschum, habilitation thesis, Stuttgart University, 1997.

[22] R. Würschum, T. Michel, P. Scharwaechter, W. Frank, and H.-E. Schaefer, Nanostruct. Mater. **12**, 555 (1999).

[23] R. Würschum, E. A. Kümmerle, K. Badura-Gergen, A. Seeger, Chr. Herzig, and H.-E. Schaefer, J. Appl. Phys. **80**, 724 (1996).

[24] C. U. Maier and H. Kronmüller, Z. Metallkd. **84**, 6 (1993).

[25] R. Würschum, P. Farber, R. Dittmar, P. Scharwaechter, W. Frank, and H.-E. Schaefer, Phys. Rev. Lett. **79**, 4918 (1997).

[26] R. Dittmar, R. Würschum, W. Ulfert, H. Kronmüller, and H.-E. Schaefer, Solid State Commun. **105**, 221 (1998).

[27] E. Shapiro, R. Würschum, H.-E. Schaefer, H. Ehrhardt, C. E. Krill, and R. Birringer, Mater. Sci. Forum **343-346**, 726 (2000).

[28] G. Trumpy and M. D. Bentzon, J. Phys.: Condens. Matter **4**, 419 (1992).

[29] R. Würschum and A. Seeger, Philos. Mag. A **73**, 1489 (1996).

[30] G. Kögel, J. Winter, and W. Triftshäuser, in *Metallic Glasses: Science and Technology*, edited by C. Hargitai, I. Bakonyi, and T. Kemény (Kultura, Budapest, 1981), p. 311.

[31] The same is also true if a lower value $H_V^F = 1.28$ eV (Ref. 6) of the vacancy-formation enthalpy with a pre-exponential factor $\sigma_V \exp(S_V^F/k_B) = 8.5 \times 10^{15}$ s^{-1} is used; see Th. Hehenkamp, Th. Kurschat, and W. Lühr-Tanck, J. Phys. F: Met. Phys. **16**, 981 (1986).

[32] J. Bernardini, P. Gas, E. D. Hondros, and M. P. Seah, Proc. R. Soc. London, Ser. A **379**, 159 (1982).

[33] R. Würschum, diploma thesis, Stuttgart University, 1985.

[34] L. Pasquini, A. Rempel, R. Würschum, K. Reimann, M. A. Müller, B. Fultz, and H.-E. Schaefer (unpublished).